MODEL ORDER REDUCTION OF ELECTROMAGNETIC DEVICES WITH A MIXED CURRENT-VOLTAGE EXCITATION

M. Nassar Albunni,[1] Rudy Eid[2] and Boris Lohmann[2]
[1]Robert Bosch GmbH, Germany, [2]Technische Universität München, Germany

Corresponding author: R. Eid, Technische Universität München, Institute for Automatic Control
Boltzmann Str. 15, 85748, Garching, Germany, eid@tum.de

Abstract. This paper deals with model reduction of linear electromagnetic devices with a mixed current-voltage excitation. For this class of systems, two models that depend on the type of excitation are required to represent the system's input-output behavior, and consequently two reduced-order models need to be generated. In this work, the input Krylov subspaces of both the voltage and current-driven models are proved to be equivalent. This equivalence allows halving the computational costs of reducing the order of both original models, by projecting them onto the same input Krylov subspace. Moreover, it significantly simplifies the procedure needed for switching the excitation signal during the device simulation using the reduced-order models. As an example, the presented results are applied to reduce the BEM-FEM models of an electrical transformer.

1 Introduction

Modeling methods that are based on the finite spatial discretization approaches, e.g. finite elements, finite volume, finite difference, have become very popular nowadays in a wide range of modeling fields. This is due to their generic nature and to their applicability to a large number of engineering problems. However, a well-known disadvantage of those modeling approaches is the high dimensionality of the generated models, which generally makes the computational cost of solving their underlying system of equations very expensive, especially if several models have to be coupled and solved simultaneously.

Model order reduction techniques present a solution for this problem, by offering the possibility of generating accurate reduced-order models that are able to approximate the behavior of the original large scale models, while being much faster in the required simulation time. Hence, by generating reduced-order models of the different components of a system, the simulation of the whole system can be performed very efficiently. One of the leading approaches in model reduction of large-scale linear dynamical system are Krylov subspace methods[1, 2, 3]. These numerically efficient methods are based on matching some of the first coefficients of the Taylor series' expansion of the transfer functions (called moments) of the original and reduced models. The reduced-order model is obtained from the original state-space one by applying a projection where the so called Krylov subspaces and numerically robust algorithms are involved.

When modeling linear electromagnetic (EM) devices with electrical excitation coils, the input-output behavior of the device's model changes significantly when switching the applied excitation signal type from voltage to current or vice versa. Accordingly, two different LTI systems are needed to model such devices: a voltage-driven model and a current-driven one. Similarly, two reduced-order models have to be generated in order to achieve a good approximation of both original models. These models are typically generated using two different Krylov subspaces as a result of the dissimilarity of the original models. This results in two different reduced-order state vectors for the current and the voltage-driven models, and imposes the need of performing a state transformation whenever the excitation signal type is changed during the device simulation.

In this paper, the generation of the two reduced-order models is carried out using the same projection matrix, based on the equivalence of the input Krylov subspaces of the voltage-driven and current-driven models respectively. In other words, it is shown that by calculating the projection matrix for the current-driven model, it is possible to reduce the order of the voltage-driven model using the same projection matrix while still guaranteeing the moment matching property. In addition, as both reduced-order models are projected into the same subspace, it is possible now to switch the excitation signal type during the simulation run without the need of performing the state transformation mentioned above. This fact, together with the need of building only one Krylov subspace, results in almost halving the generation time of the reduced-order models, and in a dramatic decrease of the simulation time when compared with the general case.

The rest of the paper is organized as follows: In the next section, the modeling of electromagnetic devices using the BEM-FEM method is presented. In section 3, Krylov-based order reduction is reviewed. In section 4, the equivalence of the input Krylov subspaces for both the voltage-driven and the current-driven models is proved. To illustrate the theoretical results, several simulations using both reduced-order models of an electrical transformer are presented in section 5.

2 Modeling of electromagnetic devices

Large-scale linear models of electromagnetic devices results in general from applying one of the finite spatial discretization methods to solve the underlying Maxwell's equations describing the device. In this context, an electromagnetic system's model is said to be linear when the relation between the magnetic field strength vector $\vec{\mathrm{H}}$ and the magnetic flux density vector $\vec{\mathrm{B}}$ can be expressed, for all the materials that are contained in the modeled device, as:

$$\vec{\mathrm{H}} = \nu \vec{\mathrm{B}}$$

where $\nu = \nu_0 \nu_r$ is the magnetic reluctivity, ν_0 is the reluctivity constant of vacuum, and ν_r is the relative magnetic reluctivity of the considered material.

Assuming that the modeled electromagnetic device can be subdivided into ℓ different regions, such that each region contains a different linear magnetic material characterized by a certain magnetic reluctivity ν_i and a certain electrical conductivity σ_i, the spatially discretized electromagnetic field BEM-FEM [4, 5] model can be written as:

$$\begin{bmatrix} \mathbf{E} & \mathbf{0} \\ \mathbf{0} & \mathbf{0} \end{bmatrix} \frac{d}{dt} \begin{bmatrix} \mathbf{a}(t) \\ \mathbf{q}(t) \end{bmatrix} + \begin{bmatrix} \mathbf{K} & -\mathbf{T} \\ \mathbf{H} & \mathbf{G} \end{bmatrix} \begin{bmatrix} \mathbf{a}(t) \\ \mathbf{q}(t) \end{bmatrix} = \begin{bmatrix} \mathbf{r}(t) \\ \mathbf{r}_\gamma(t) \end{bmatrix}, \tag{1}$$

where the global damping matrix $\mathbf{E}$ and the global stiffness matrix $\mathbf{K}$ can be calculated respectively as a sum of the individual matrices in the different subregions:

$$\begin{aligned} \mathbf{E} &= \sum_{i=1}^{\ell} \sigma_1 \mathbf{E}_1 + \cdots + \sigma_i \mathbf{E}_i, \\ \mathbf{K} &= \sum_{i=1}^{\ell} \nu_1 \mathbf{K}_1 + \cdots + \nu_i \mathbf{K}_i. \end{aligned} \tag{2}$$

The model (1) is a dynamical system with a high number of differential algebraic equations (DAE), often called descriptor or singular state-space system in the control engineering community. Such systems represent a real challenge for applying model order reduction and very few methods, which are mainly based on transforming the system to some special canonical forms, exist. In this work, the singularity problem in (1) is tackled by eliminating the algebraic equations through solving for $\mathbf{q}(t)$:

$$\mathbf{q}(t) = -\mathbf{G}^{-1}\mathbf{H}\mathbf{a}(t) + \mathbf{G}^{-1}\mathbf{r}_\gamma(t),$$

and substituting it back in (1),

$$\mathbf{E}\dot{\mathbf{a}}(t) + \left[\mathbf{K} + \mathbf{K}^{\mathrm{BEM}}\right]\mathbf{a}(t) = \mathbf{r}(t) + \mathbf{T}\mathbf{G}^{-1}\mathbf{r}_\gamma(t), \tag{3}$$

with

$$\mathbf{K}^{\mathrm{BEM}} = \mathbf{T}\mathbf{G}^{-1}\mathbf{H}.$$

The matrix $\mathbf{K}^{\mathrm{BEM}}$ is called the boundary matrix which remains constant when modeling electromagnetic devices with non-moving components. The input signal $\mathbf{r}_\gamma(t)$ corresponds to the contribution of the field sources that are located in vacuum and not included in the spatial discretization. However, in this work, it is assumed that all sources of electromagnetic field can be included in the vector $\mathbf{r}(t)$, leading to $\mathbf{r}_\gamma(t) = \mathbf{0}$. Even though several outputs can be calculated as function of the state variables of the large-scale linear system (1), in this section, the considered outputs are those that can be calculated as a linear combination of the state variables,

$$y(t) = \mathbf{l}^T \mathbf{a}(t), \tag{4}$$

where $\mathbf{l}^T$ is the system output vector. It should be noted that the algebraic variables $\mathbf{q}(t)$ do not directly contribute in general to the typical linear output functions of electromagnetic systems.

The sources of EM field excitation are electrical coils with homogenous current densities through out their cross sections. Thus, depending on the applied excitation signals, i.e. voltage or current, two variant formulations for the models (3) can be derived.

2.1 Current-driven model

Under the assumption that the modeled EM device contains m different excitation coils connected to m different current sources $i_1(t), \ldots, i_m(t)$, the linear model (3) can be written as:

$$\mathbf{E}^c\dot{\mathbf{a}}(t) + \left[\mathbf{K} + \mathbf{K}^{BEM}\right]\mathbf{a}(t) = \begin{bmatrix} \mathbf{b}_1 & \ldots & \mathbf{b}_m \end{bmatrix} \begin{bmatrix} i_1(t) \\ \vdots \\ i_m(t) \end{bmatrix}, \tag{5}$$

where each of the vectors $\mathbf{b}_i \in \mathbb{R}^n$ describes the distribution of the current density in the i-th excitation coil. The transfer function matrix describing the input-output behavior from each of the m inputs to any linear output of the form $y(t) = \mathbf{l}^T \mathbf{a}$, can be written as:

$$\mathbf{G}^c(s) = \mathbf{l}^T \left(s\mathbf{E}^c - \mathbf{A}\right)^{-1} \mathbf{B}. \tag{6}$$

with $\mathbf{B} = [\mathbf{b}_1 \ \ldots \ \mathbf{b}_m]$, and $\mathbf{A} = \left(\mathbf{K} + \mathbf{K}^{BEM}\right)$.

2.2 Voltage-driven model

Now, if all the excitation coils of the modeled EM device are connected to voltage sources, the value of the current $i_k(t)$ flowing in the k-th excitation coil can be calculated as [6]:

$$i_k(t) = \mathbf{b}_k^T \dot{\mathbf{a}}(t) - \frac{u_k(t)}{R_k}, \tag{7}$$

where R_k is the Ohmic resistance of the k-th excitation coil, and $u_k(t)$ is the voltage signal applied to its terminals. By substituting the excitation currents values from (7) in (5) and assuming that $\tilde{\mathbf{B}} = \left[\frac{\mathbf{b}_1}{R_1}, \quad \ldots \quad , \frac{\mathbf{b}_m}{R_m}\right]$, the formulation of the current driven EM field model is found to be:

$$\left[\mathbf{E}^c + \mathbf{B}\tilde{\mathbf{B}}^T\right] \dot{\mathbf{a}}(t) + \left[\mathbf{K} + \mathbf{K}^{BEM}\right] \mathbf{a}(t) = \tilde{\mathbf{B}} \begin{bmatrix} u_1(t) \\ \vdots \\ u_m(t) \end{bmatrix}., \tag{8}$$

with its transfer function

$$\mathbf{G}^v(s) = \mathbf{l}^T \left(s\mathbf{E}^v - \mathbf{A}\right)^{-1} \tilde{\mathbf{B}}, \tag{9}$$

where $\mathbf{E}^v = \left(\mathbf{E}^c + \mathbf{B}\tilde{\mathbf{B}}^T\right)$.

3 Krylov-based model order reduction

Consider the continuous-time dynamical system in state-space,

$$\begin{cases} \mathbf{E}\dot{\mathbf{x}}(t) = \mathbf{A}\mathbf{x}(t) + \mathbf{B}\mathbf{u}(t), \\ \mathbf{y}(t) = \mathbf{C}\mathbf{x}(t), \end{cases} \tag{10}$$

where $\mathbf{E}, \mathbf{A} \in \mathbb{R}^{n\times n}$, $\mathbf{B} \in \mathbb{R}^{n\times m}$, $\mathbf{C} \in \mathbb{R}^{p\times n}$ are the constant system's matrices, $\mathbf{u}(t) \in \mathbb{R}^m$, $\mathbf{y}(t) \in \mathbb{R}^p$, $\mathbf{x}(t) \in \mathbb{R}^n$ are respectively the input, output and states vectors of the system.

The transfer function of the system (10) in the Laplace domain is then:

$$\mathbf{H}(s) = \mathbf{C}(s\mathbf{E} - \mathbf{A})^{-1}\mathbf{B},$$

with its moments about zero calculated as follows [1]:

$$\mathbf{m}_i = \mathbf{C}\left(\mathbf{A}^{-1}\mathbf{E}\right)^i \mathbf{A}^{-1}\mathbf{B}, \quad i = 0, 1, \cdots. \tag{11}$$

By replacing s in the transfer matrix with the shifted variable $(s - s_0)$,

$$\mathbf{H}(s) = \mathbf{C}[(s - s_0)\mathbf{E} - (\mathbf{A} - s_0\mathbf{E})]^{-1}\mathbf{B}, \tag{12}$$

the moments about s_0 can be computed by replacing $\mathbf{A}$ by $(\mathbf{A} - s_0\mathbf{E})$ in (11) (assuming that $(\mathbf{A} - s_0\mathbf{E})$ is nonsingular),

$$\mathbf{m}_i^{s_0} = \mathbf{C}((\mathbf{A} - s_0\mathbf{E})^{-1}\mathbf{E})^i(\mathbf{A} - s_0\mathbf{E})^{-1}\mathbf{B} \quad i = 0, 1, \cdots. \tag{13}$$

The aim of order reduction by moment matching is to find a reduced-order model of order $q \ll n$, whose moments match some of those of the original one [1, 2, 7]. When some of the moments about $s = 0$ are matched, the reduced-order model is known as Padé approximant. For the case of $s = s_0$, we speak about a shifted Padé approximant.

A numerically robust and efficient way to calculate this reduced model is based on applying a projection to the original model of the form,

$$\mathbf{x} = \mathbf{V}\mathbf{x}_r, \quad \mathbf{V} \in \mathbb{R}^{n\times q}, \ \mathbf{x} \in \mathbb{R}^n, \ \mathbf{x}_r \in \mathbb{R}^q, \tag{14}$$

and multiplying the state equation by the transpose of a matrix $\mathbf{W} \in \mathbb{R}^{n\times q}$. Accordingly, the following model with a reduced order q is found:

$$\begin{cases} \mathbf{W}^T\mathbf{E}\mathbf{V}\dot{\mathbf{x}}_r(t) = \mathbf{W}^T\mathbf{A}\mathbf{V}\mathbf{x}_r(t) + \mathbf{W}^T\mathbf{B}\mathbf{u}(t), \\ \mathbf{y}(t) = \mathbf{C}\mathbf{V}\mathbf{x}_r(t). \end{cases}$$

leading to the reduced-system's matrices:

$$\mathbf{E}_r = \mathbf{W}^T\mathbf{E}\mathbf{V},\ \ \mathbf{A}_r = \mathbf{W}^T\mathbf{A}\mathbf{V},\ \ \mathbf{B}_r = \mathbf{W}^T\mathbf{B},\ \ \mathbf{C}_r = \mathbf{C}\mathbf{V},$$

For the choice of the projection matrices $\mathbf{V}$ and $\mathbf{W}$, the Krylov subspace, defined in e.g. [1] is used,

$$\mathscr{K}_q(\mathbf{A}_1, \mathbf{b}_1) = span\{\mathbf{b}_1, \mathbf{A}_1\mathbf{b}_1, \cdots, \mathbf{A}_1^{q-1}\mathbf{b}_1\}$$

where $\mathbf{A}_1 \in \mathbb{R}^{n\times n}$, and $\mathbf{b}_1 \in \mathbb{R}^n$ is called the starting vector.

It can be shown that if the projection matrices are chosen such that,

$$colspan(\mathbf{V}) \subset \mathscr{K}_{q_1}\left((\mathbf{A}-s_0\mathbf{E})^{-1}\mathbf{E}, (\mathbf{A}-s_0\mathbf{E})^{-1}\mathbf{B}\right),$$
$$colspan(\mathbf{W}) \subset \mathscr{K}_{q_2}\left((\mathbf{A}-s_0\mathbf{E})^{-T}\mathbf{E}^T, (\mathbf{A}-s_0\mathbf{E})^{-T}\mathbf{C}^T\right),$$

then $\frac{q}{m} + \frac{q}{p}$ moments about s_0 match and the method is called a two-sided Krylov method [1, 2]. Note that in the MIMO case, for the projection matrices $\mathbf{V}$ and $\mathbf{W}$ to have the appropriate dimensions, the order of the reduced system, i.e. the rank of the projection matrices should be a common multiple of the number of inputs and outputs.

In the so-called one-sided method, only one Krylov subspace is used with a common choice $\mathbf{W} = \mathbf{V}$ and only $\frac{q}{m}$ or $\frac{q}{p}$ moments match.

For the numerical computation of the matrices $\mathbf{V}$ and $\mathbf{W}$, the known Lanczos or Arnoldi or one of their modified versions are employed. For more details, see e.g. [1] and the references therein.

4 Order reduction of EM devices with mixed excitation

In comparison to the order of the model (1), the model (3) has been already reduced, due to the elimination of the algebraic variable $\mathbf{q}(t)$. However, it is still a large-scale model, whose order reduction is still meaningful and of high interest. In this section, Krylov-based model reduction techniques are applied for the reduction of both the current and voltage-driven models, and the connection between the involved Krylov subspaces, and subsequently, the resulting reduced-order model, is investigated.

4.1 Order reduction of the current-driven model

By expanding the transfer function (6) as a Laurent series about a given point s_0, its moments can be calculated. Setting $\mathbf{A}^c_{s_0} = (\mathbf{A} - s_0\mathbf{E}^c)$, the expanded transfer function can be rewritten as:

$$\mathbf{G}^c(s) = \mathbf{l}^T\left(\mathbf{A}^c_{s_0}\right)^{-1}\mathbf{B} + \mathbf{l}^T\left(\mathbf{A}^c_{s_0}\right)^{-1}\mathbf{E}^c\left(\mathbf{A}^c_{s_0}\right)^{-1}\mathbf{B}(s-s_0) + \mathbf{l}^T\left(\left(\mathbf{A}^c_{s_0}\right)^{-1}\mathbf{E}^c\right)^2\left(\mathbf{A}^c_{s_0}\right)^{-1}\mathbf{B}(s-s_0)^2 + \ldots$$
$$+ \mathbf{l}^T\left(\left(\mathbf{A}^c_{s_0}\right)^{-1}\mathbf{E}^c\right)^{q-1}\left(\mathbf{A}^c_{s_0}\right)^{-1}\mathbf{B}(s-s_0)^{q-1} + \ldots$$

leading to the general expression of the moments of the system (5),

$$\mathbf{m}^c_i = \mathbf{l}^T\left((\mathbf{A}^c_{s_0})^{-1}\mathbf{E}^c\right)^i(\mathbf{A}^c_{s_0})^{-1}\mathbf{B} \quad i = 0, 1, \cdots. \tag{15}$$

Now, based on the previous section and equation (15), the system (5) can be reduced from order n to order $q << n$ using a one-sided Krylov subspace method where the columns of the projection matrix $\mathbf{V}$ span the following subspace:

$$\mathscr{K}^c_{q_1}\left(\left(\mathbf{A}^c_{s_0}\right)^{-1}\mathbf{E}^c, \left(\mathbf{A}^c_{s_0}\right)^{-1}\mathbf{B}\right) = span\left\{\left(\mathbf{A}^c_{s_0}\right)^{-1}\mathbf{B}, \left((\mathbf{A}^c_{s_0})^{-1}\mathbf{E}^c\right)(\mathbf{A}^c_{s_0})^{-1}\mathbf{B}, \ldots, \left((\mathbf{A}^c_{s_0})^{-1}\mathbf{E}^c\right)^{q-1}(\mathbf{A}^c_{s_0})^{-1}\mathbf{B}\right\} \tag{16}$$

This choice guarantees the matching of the first $\frac{q}{m}$ moments of the transfer functions of the original and reduced models. Accordingly, the resulting current-driven reduced-order model can be calculated by replacing the original state vector $\mathbf{a}$ in (5) by its approximated value $\mathbf{a} \approx \mathbf{V}_c\mathbf{a}^c_r$ as follows:

$$\mathbf{V}_c^T\mathbf{E}^c\mathbf{V}_c\dot{\mathbf{a}}^c_r(t) + \mathbf{V}_c^T\left[\mathbf{K} + \mathbf{K}^{BEM}\right]\mathbf{V}_c\mathbf{a}^c_r(t) = \mathbf{V}_c^T\mathbf{B}\begin{bmatrix} i_1(t) \\ \vdots \\ i_m(t)\end{bmatrix}, \tag{17}$$

with $colspan(\mathbf{V}_c) \subset \mathscr{K}^c_{q_1}$.

4.2 Order reduction of the voltage-driven model

Similar to the current-driven model case, and by setting $\mathbf{A}^v_{s_0} = \left(\mathbf{A} - s_0\mathbf{E}^c - s_0\mathbf{B}\tilde{\mathbf{B}}^T\right)$ the transfer function of the voltage-driven model expanded about s_0 can be shown to be:

$$\begin{aligned}\mathbf{G}^v(s) = \mathbf{l}^T\left(\mathbf{A}^v_{s_0}\right)^{-1}\tilde{\mathbf{B}} \;+\; \mathbf{l}^T\left(\mathbf{A}^v_{s_0}\right)^{-1}\mathbf{E}^v\left(\mathbf{A}^v_{s_0}\right)^{-1}\tilde{\mathbf{B}}(s-s_0) \;+\; \mathbf{l}^T\left(\left(\mathbf{A}^v_{s_0}\right)^{-1}\mathbf{E}^v\right)^2\left(\mathbf{A}^v_{s_0}\right)^{-1}\mathbf{B}(s-s_0)^2+\ldots\\ +\; \mathbf{l}^T\left(\left(\mathbf{A}^c_{s_0}\right)^{-1}\mathbf{E}^v\right)^{q-1}\left(\mathbf{A}^v_{s_0}\right)^{-1}\tilde{\mathbf{B}}(s-s_0)^{q-1} \;+\; \ldots\end{aligned}$$

Accordingly, the moments of this system can be calculated as:

$$\mathbf{m}^v_i = \mathbf{l}^T\left((\mathbf{A}^v_{s_0})^{-1}\mathbf{E}^v\right)^i(\mathbf{A}^v_{s_0})^{-1}\tilde{\mathbf{B}} \quad i = 0,1,\cdots. \tag{18}$$

Hence, the voltage-driven model (8) can be reduced by projection in a similar way to the current-driven model using the following Krylov subspace:

$$\mathscr{K}^v_{q_1}\left(\left(\mathbf{A}^v_{s_0}\right)^{-1}\mathbf{E}^v, \left(\mathbf{A}^v_{s_0}\right)^{-1}\tilde{\mathbf{B}}\right) = span\left\{\left(\mathbf{A}^v_{s_0}\right)^{-1}\tilde{\mathbf{B}}, \left((\mathbf{A}^v_{s_0})^{-1}\mathbf{E}^v\right)(\mathbf{A}^v_{s_0})^{-1}\tilde{\mathbf{B}}, \ldots, \left((\mathbf{A}^v_{s_0})^{-1}\mathbf{E}^v\right)^{q_1-1}(\mathbf{A}^v_{s_0})^{-1}\tilde{\mathbf{B}}\right\} \tag{19}$$

This choice guarantees the matching of the first $\frac{q}{m}$ moments of the transfer functions of the original and reduced models. Accordingly, the resulting voltage-driven reduced-order model can be calculated by replacing the original state vector $\mathbf{a}$ in (8) by its approximated value $\mathbf{a} \approx \mathbf{V}_v\mathbf{a}^v_r$ as follows:

$$\mathbf{V}_v^T\left[\mathbf{E}^c + \mathbf{B}\tilde{\mathbf{B}}^T\right]\mathbf{V}_v\dot{\mathbf{a}}^v_r(t) + \mathbf{V}_v^T\left[\mathbf{K} + \mathbf{K}^{BEM}\right]\mathbf{V}_v\mathbf{a}^v_r(t) = \mathbf{V}_v^T\tilde{\mathbf{B}}\begin{bmatrix}u_1(t)\\ \vdots \\ u_m(t)\end{bmatrix}, \tag{20}$$

with $colspan(\mathbf{V}_v) \subset \mathscr{K}^v_{q_1}$.

4.3 The equivalence of the input Krylov subspaces

As they involve different matrices and vectors, the input Krylov subspaces (16) and (19) employed in the reduction of the current and voltage-driven models seem to be different. However, by closely examining the connections between the involved matrices and vectors it can be shown that these two subspaces are equal when calculated at the same expansion point s_0.

Theorem 1. *The input Krylov subspaces of the current-driven model $\mathscr{K}^c_{q_1}$ and that of the voltage-driven model $\mathscr{K}^v_{q_1}$ are equal.*

Proof. Let $\mathbf{M}_i$ and $\mathbf{N}_i$ be the basic blocks of the Krylov subspace $\mathscr{K}^c_{q_1}$ and $\mathscr{K}^v_{q_1}$ respectively. It is shown that the two subspaces span the same space by proving that the i-th basic block of the second one can be written as a linear combination of the first i blocks of the first one.

Recall the *Woodbury formula* [8] employed generally to reformulate the inverse of the sum of two matrices,

$$(\mathbf{M}+\mathbf{PQ})^{-1} = \mathbf{M}^{-1} - \mathbf{M}^{-1}\mathbf{P}\left(\mathbf{I}+\mathbf{QM}^{-1}\mathbf{P}\right)^{-1}\mathbf{QM}^{-1},$$

where $\mathbf{M} \in \mathbb{R}^{n\times n}$ is an arbitrary invertible matrix and $\mathbf{P} \in \mathbb{R}^{n\times m}$, $\mathbf{Q} \in \mathbb{R}^{m\times n}$ are arbitrary matrices. Applying this formula to inverse the matrix $\mathbf{A}^v_{s_0}$ in (19) results in:

$$\begin{aligned}\left(\mathbf{A}^v_{s_0}\right)^{-1} &= \left(\mathbf{A}^c_{s_0} - s_0\mathbf{B}\tilde{\mathbf{B}}^T\right)^{-1} = \left(\mathbf{A}^c_{s_0}\right)^{-1} - s_0\left(\mathbf{A}^c_{s_0}\right)^{-1}\mathbf{B}\left(\mathbf{I}+s_0\tilde{\mathbf{B}}^T\left(\mathbf{A}^c_{s_0}\right)^{-1}\mathbf{B}\right)^{-1}\tilde{\mathbf{B}}^T\left(\mathbf{A}^c_{s_0}\right)^{-1}\\ &= \left(\mathbf{A}^c_{s_0}\right)^{-1} - s_0\left(\mathbf{A}^c_{s_0}\right)^{-1}\mathbf{B}\mathbf{D}_{s_0}\tilde{\mathbf{B}}^T\left(\mathbf{A}^c_{s_0}\right)^{-1}, \quad \text{where } \mathbf{D}_{s_0} = \left(\mathbf{I}+s_0\tilde{\mathbf{B}}^T\left(\mathbf{A}^c_{s_0}\right)^{-1}\mathbf{B}\right)^{-1} \in \mathbb{R}^{m\times m}.\end{aligned} \tag{21}$$

The starting vectors block of the input Krylov subspace (16) of the current-driven model is given by:

$$\mathbf{M}_1 = \left(\mathbf{A}^c_{s_0}\right)^{-1}\mathbf{B}.$$

The starting vectors block for the subspace (19) of the voltage driven model is given by:

$$\begin{aligned}\mathbf{N}_1 = \left(\mathbf{A}^c_{s_0} - s_0\mathbf{B}\tilde{\mathbf{B}}^T\right)^{-1}\tilde{\mathbf{B}} &= \left(\mathbf{A}^c_{s_0}\right)^{-1}\tilde{\mathbf{B}} - s_0\left(\mathbf{A}^c_{s_0}\right)^{-1}\mathbf{B}\mathbf{D}_{s_0}\tilde{\mathbf{B}}^T\left(\mathbf{A}^c_{s_0}\right)^{-1}\tilde{\mathbf{B}}\\ &= \left(\mathbf{A}^c_{s_0}\right)^{-1}\mathbf{B}\Phi_1 = \mathbf{M}_1\Phi_1.\end{aligned}$$

where $\Phi_1 = \left(diag\left(\left[\frac{1}{R_1},\ldots,\frac{1}{R_m}\right]\right) - s_0\mathbf{D}_{s_0}\tilde{\mathbf{B}}^T\left(\mathbf{A}_{s_0}^c\right)^{-1}\tilde{\mathbf{B}}\right) \in \mathbb{R}^{m\times m}$. The second vectors block of the input Krylov subspace (19) is given by:

$$\begin{aligned}
\mathbf{N}_2 &= \left(\left(\mathbf{A}_{s_0}^c\right)^{-1} - s_0\mathbf{B}\tilde{\mathbf{B}}^T\right)^{-1}\left(\mathbf{E}^c + \mathbf{B}\tilde{\mathbf{B}}^T\right)\left(\mathbf{A}_{s_0}^c - s_0\mathbf{B}\tilde{\mathbf{B}}^T\right)^{-1}\tilde{\mathbf{B}} \\
&= \left(\left(\mathbf{A}_{s_0}^c\right)^{-1} - s_0\left(\mathbf{A}_{s_0}^c\right)^{-1}\mathbf{B}\mathbf{D}_{s_0}\tilde{\mathbf{B}}^T\left(\mathbf{A}_{s_0}^c\right)^{-1}\right)\left(\mathbf{E}^c + \mathbf{B}\tilde{\mathbf{B}}^T\right)\left(\mathbf{A}_{s_0}^c\right)^{-1}\mathbf{B}\Phi_1 \\
&= \left(\mathbf{A}_{s_0}^c\right)^{-1}\mathbf{E}^c\left(\mathbf{A}_{s_0}^c\right)^{-1}\mathbf{B}\Phi_1 - \left(\mathbf{A}_{s_0}^c\right)^{-1}\mathbf{B}\mathbf{D}_{s_0}\tilde{\mathbf{B}}^T\tilde{\mathbf{A}}_{s_0}^{-1}\mathbf{E}^c\left(\mathbf{A}_{s_0}^c\right)^{-1}\mathbf{B}\Phi_1 s_0 + \left(\mathbf{A}_{s_0}^c\right)^{-1}\mathbf{B}\tilde{\mathbf{B}}^T\left(\mathbf{A}_{s_0}^c\right)^{-1}\mathbf{B}\Phi_1 \\
&\quad - \left(\mathbf{A}_{s_0}^c\right)^{-1}\mathbf{B}\mathbf{D}_{s_0}\tilde{\mathbf{B}}^T\left(\mathbf{A}_{s_0}^c\right)^{-1}\mathbf{B}\tilde{\mathbf{B}}^T\left(\mathbf{A}_{s_0}^c\right)^{-1}\mathbf{B}\Phi_1 s_0 \\
&= \left(\mathbf{A}_{s_0}^c\right)^{-1}\mathbf{E}^c\left(\mathbf{A}_{s_0}^c\right)^{-1}\mathbf{B}\Phi_1 + \left(\mathbf{A}_{s_0}^c\right)^{-1}\mathbf{B}\Phi_2 \\
&= \mathbf{M}_2\Phi_1 + \mathbf{M}_1\Phi_2
\end{aligned}$$

with $\Phi_2 = \left(-\mathbf{D}_{s_0}\tilde{\mathbf{B}}^T\left(\mathbf{A}_{s_0}^c\right)^{-1}\mathbf{E}^c\left(\mathbf{A}_{s_0}^c\right)^{-1}\mathbf{B}\Phi_1 s_0 + \tilde{\mathbf{B}}^T\left(\mathbf{A}_{s_0}^c\right)^{-1}\mathbf{B}\Phi_1 - \mathbf{D}_{s_0}\tilde{\mathbf{B}}^T\left(\mathbf{A}_{s_0}^c\right)^{-1}\mathbf{B}\tilde{\mathbf{B}}^T\left(\mathbf{A}_{s_0}^c\right)^{-1}\mathbf{B}\Phi_1 s_0\right) \in \mathbb{R}^{m\times m}$.

Now consider that $\mathbf{N}_{q-1} = \mathbf{M}_{q-1}\Phi_1 + \cdots + \mathbf{M}_1\Phi_{q-1}$, for $\mathbf{N}_q$ we have:

$$\begin{aligned}
\mathbf{N}_q &= \left(\left(\tilde{\mathbf{A}}_{s_0} - s_0\mathbf{B}\tilde{\mathbf{B}}^T\right)^{-1}\left(\mathbf{E}^c + \mathbf{B}\tilde{\mathbf{B}}^T\right)\right)\mathbf{N}_{q-1} \\
&= \left(\left(\mathbf{A}_{s_0}^c\right)^{-1} - s_0\left(\mathbf{A}_{s_0}^c\right)^{-1}\mathbf{B}\mathbf{D}_{s_0}\tilde{\mathbf{B}}^T\left(\mathbf{A}_{s_0}^c\right)^{-1}\right)\left(\mathbf{E}^c + \mathbf{B}\tilde{\mathbf{B}}^T\right)\left(\mathbf{M}_{q-1}\Phi_1 + \cdots + \mathbf{M}_1\Phi_{q-1}\right) \\
&= \left(\mathbf{A}_{s_0}^c\right)^{-1}\mathbf{E}^c\mathbf{V}_{q-1}\Phi_1 + \cdots + \left(\mathbf{A}_{s_0}^c\right)^{-1}\mathbf{E}^c\mathbf{M}_1\Phi_{q-1} + \left(\mathbf{A}_{s_0}^c\right)^{-1}\mathbf{B}\tilde{\mathbf{B}}\left(\mathbf{M}_{q-1}\Phi_1 + \cdots + \mathbf{M}_1\Phi_{q-1}\right) \\
&\quad - \left(\mathbf{A}_{s_0}^c\right)^{-1}\mathbf{B}\mathbf{D}_{s_0}\tilde{\mathbf{B}}^T\left(\mathbf{A}_{s_0}^c\right)^{-1}\left(\mathbf{E}^c + \mathbf{B}\tilde{\mathbf{B}}^T\right)\left(\mathbf{M}_{q-1}\Phi_1 + \cdots + \mathbf{M}_1\Phi_{q-1}\right)s_0 \\
&= \mathbf{M}_q\Phi_1 + \mathbf{M}_{q-1}\Phi_2 + \cdots + \mathbf{M}_1\Phi_q.
\end{aligned}$$

The proof is completed by induction. □

Remark 1. *The presented proof considers the most general case of MIMO systems with an expansion point $s_0 \neq 0$. The subspaces of Theorem 1 are also equal for the SISO case and/or $s_0 = 0$.*

Consequently, the order of both the voltage-driven and the current-driven models can be reduced using the same input Krylov subspace, e.g. (16), while still guaranteeing the matching of the first $\frac{q}{m}$ moments between each of the original models and their corresponding reduced ones.

In order to further illustrate the advantages of the presented equivalence, it is assumed that the response of a linear electromagnetic device to a given voltage signal is simulated using the voltage-driven reduced-order model (20). During the time interval $[t_0, t_s]$, the value of the state vector evolves from its initial value to a new value $\mathbf{a}_r^v(t_s)$. At the time point t_s, the excitation signal is switched from voltage to current and the simulation has to be continued using the current-driven reduced-order model (17). However, in order to calculate the initial conditions $\mathbf{a}_r^c(t_s)$, the current state $\mathbf{a}_r^v(t_s)$ of the device's model has to be projected onto the subspace of the current-driven model. This can be done by first projecting $\mathbf{a}_r^v(t_s)$ back onto the full order space, $\mathbf{a}(t_s) \approx \mathbf{V}_v\mathbf{a}_r^v(t_s)$ and then projecting the result onto the subspace of the current-driven model, $\mathbf{a}_r^c(t_s) \approx \mathbf{V}_c^T\mathbf{V}_v\mathbf{a}_r^v(t_s)$. It is clear at this point that the transformation between the subspaces is accompanied with an approximation error as the back projection on the full order subspace does not reproduce the exact high-order state vector. Moreover, the transformation matrices matrices $\mathbf{V}_c^T\mathbf{V}_v$ and $\mathbf{V}_v^T\mathbf{V}_c$ have to be saved and loaded during the simulation. In contrast, the presented proof enables projecting both models (5) and (8) onto the same subspace, leading to $\mathbf{a}_r^c(t_s) = \mathbf{a}_r^v(t_s)$.

5 Technical example

In this section, the results presented in this work are employed to apply order reduction and thus perform a fast simulation for the behavior of the electromagnetic field in the electrical transformer shown in Fig. 1. The transformer circuit contains beside the transformer itself, a voltage source and a current limiter. The resistors R_1 and R_2 represent respectively the Ohmic resistances of the primary and secondary transformer coils. The terminals of the secondary coil in this example are not connected to a load, i.e. $i_2(t) = 0$. This results in an electromagnetic system having only one excitation coil, and consequently one input, i.e. $m = 1$.

The current limiter is only activated when the absolute value of the primary current $i_1(t)$ reaches the maximum allowed value i_{max}. During its activation, it adjusts the terminal voltage $u_1(t)$ of the primary coil in order to avoid that the primary current exceeds i_{max}, as follows:

$$\begin{cases} i_1 = +i_{max}, & \text{if } i_1 > i_{max}, \\ i_1 = -i_{max}, & \text{if } i_1 < -i_{max}. \end{cases} \tag{22}$$

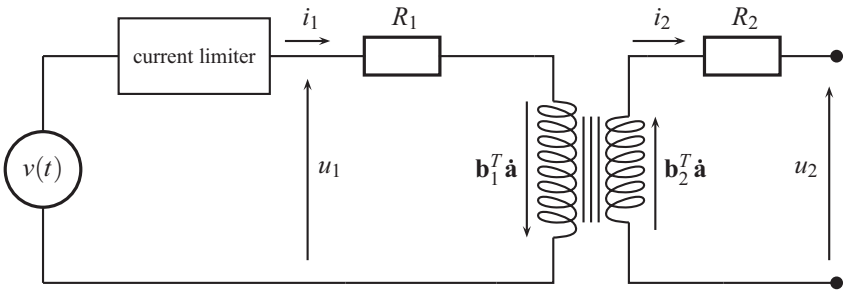

Figure 1: Electrical circuit containing an electrical transformer, a current limiter, and a voltage source $v(t)$.

The simplest and most common way to model the influence of the current limiter on the behavior of the transformer circuit is to consider it, in its activation intervals, as a constant current source, i.e. $i_1 = \pm i_{max}$. Therefore, the excitation signal has to be switched from a voltage signal to a current signal in the time intervals during which the current limiter is activated. Now, in the time intervals during which the current limiter is not activated, it passes the voltage signal generated by the voltage source directly to the primary coil, i.e. $u_1(t) = v(t)$.

A spatially discretized model of the electromagnetic field in the electrical transformer is generated using the coupled BEM-FEM method. The generated model is a high dimensional system of differential algebraic equations DAEs (1) of order $n = 3186$. The singularity of the system is handled by eliminating the algebraic part. This in turn transforms the DAEs system (1) to a system of ordinary differential equations (3) of order $n = 2614$. All the magnetic materials that are included in the transformer model are assumed to have linear magnetic properties. An input Krylov subspace (16) of the current driven model (5) is generated using the Arnoldi algorithm at the expansion point $s_0 = 0$. Both the current-driven model (5) and the voltage-driven one (8) are reduced using a one-sided method ($\mathbf{V} = \mathbf{W}$) from order $n = 2614$ to order $n = 20$ by the same projection matrices calculated from the input Krylov subspace generated in the previous step. This in turn guarantees the matching of the first 20 moments between the transfer functions of the full order models (5) and (8), and their corresponding reduced-order models as proven in the previous section.

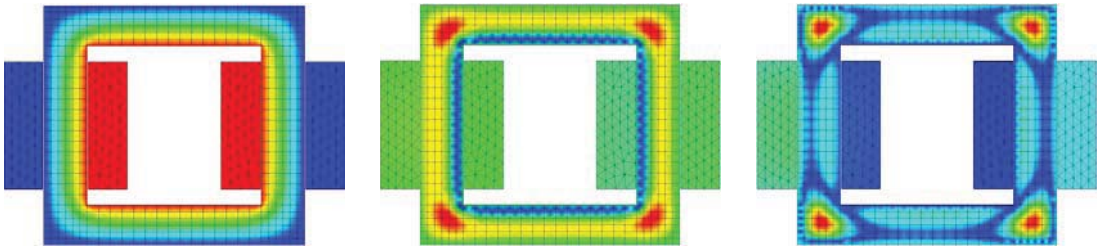

(a) First vector (b) Second vector (c) Third vector

Figure 2: The figures (a)-(c) illustrate the electromagnetic field distribution that corresponds to the first three vectors of the input Krylov subspace of the current-driven transformer model

We remind at this point that the common aim of model order approaches is to approximate the original state vector of a system by a linear combination of a low number of optimally chosen basis vectors, i.e. $\mathbf{a} = \mathbf{V}\mathbf{a}_r$. In the considered example, this means that the original distribution of the electromagnetic field in the electrical transformer can be approximated in the reduced-order models by a weighted combinations of the twenty vectors of the input Krylov subspace. Hence it is interesting to illustrate some of those basis vectors. In Figure 2, the electromagnetic field distributions corresponding to the first three vectors of the involved Krylov subspace are graphically illustrated.

After generating the reduced-order models, their performance is validated by comparing the corresponding simulation results to the ones obtained by the original high-order models. The first simulation run is carried out using the full order models (8) and (5). At the beginning, the simulation run is started using the voltage driven model (8) with the input voltage signal being equal to $u_1(t) = v(t) = 100\sin 2000t$, as shown in Fig. 3. During the progress of simulation, the value of the primary current starts to rise until it reaches the maximum allowed current value $i_{max} = 4\text{A}$. At this point, the current limiter is activated and starts maintaining the primary current value at its maximum allowed value $i_1 = i_{max}$. Therefore, the simulation is continued from this point on using the current-driven model (5) with an input signal amplitude of $i_1 = 4\text{A}$. The last value of the state vector $\mathbf{a}(t)$ is used as an initial conditions for simulating the current-driven model, as both models have the same states. The simulation is switched back again to the voltage-driven model as soon as the value of the sinusoidal voltage signal $v(t)$ becomes smaller than the terminal voltage $u_1(t)$ of the primary coil. The switching cycle from voltage to current and vice versa is repeated according to the aforementioned switching algorithm until the end of the simulation, as shown in Fig. (3). The second simulation run is performed using the generated reduced-order electromagnetic field models. The switching logic between the reduced-order voltage-driven and current-driven models is carried out according

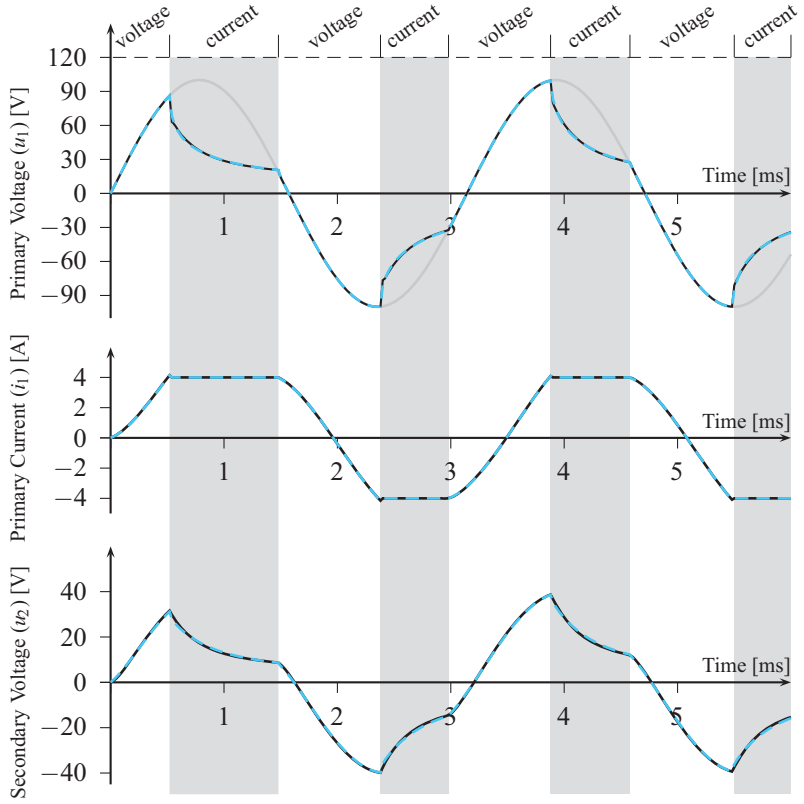

Figure 3: A comparison between the simulation results of the full order electromagnetic field models $n = 3186$ (solid lines) and the reduced-order models $n = 20$ (dashed lines). The shaded regions represent the intervals during which the simulation is carried out using the current-driven model, whereas the other regions represent the intervals during which the simulation is performed using the voltage-driven model. The gray line represents the signal of the voltage source $v(t)$.

to the same switching algorithm used for the full order models. At each switching point between the voltage and the current-driven models, the current value of the reduced-order state vector $\mathbf{a}_r(t)$ is used as an initial condition for solving the model equations in the next simulation step. No coordinate transformation is required at this point, as both the current-driven and the voltage-driven models are projected to the same subspace. This is in fact one of the major benefits of the results presented in this paper. Finally, the simulation results using the reduced models

	Full Order Models	Reduced-Order Models
order	$n = 3186$	$n = 20$
number of simulation steps	300	300
simulation step size	20 μsec	20 μsec
simulation time	127.43 sec	0.1451sec

Table 1: Simulation parameters of the full and reduced-order electromagnetic field models

that are illustrated in Fig. (3) show that the model of order $n = 20$ produces an excellent approximation of the simulation results using the original high order model of order $n = 3186$, while being almost 900 times faster as listed in Table 1.

6 Conclusions

In this paper, Krylov-based model order reduction of electromagnetic devices with a mixed current-voltage has been presented. It was shown that the input Krylov subspaces involved in the reduction of the voltage and current-driven models are equal. This reduces, almost by half, the computational cost of calculating both reduced models and simplifies and accelerates the simulation process where it is mandatory to switch between the excitation signals. Finally, based on the known analogous quantities between the mechanical and electrical systems, it would be interesting to generalize the results of this work to a larger class of systems.

7 References

[1] A. C. Antoulas. *Approximation of Large-Scale Dynamical Systems*. SIAM, Philadelphia, 2005.
[2] R. W. Freund. Model reduction methods based on Krylov subspaces. *Acta Numerica*, 12:267–319, 2003.
[3] E. J. Grimme. *Krylov Projection Methods for Model Reduction*. Ph.D thesis, Dep. of Electrical Eng., University of Illinois at Urbana Champaign, 1997.
[4] S. Kurz. *Die numerische Behandlung elektromagnetischer Systeme mit Hilfe der Kopplung der Methode der finite Elemente und der Rand Elemente*. PhD thesis, Universität Stuttgart, 1998.
[5] O. Rain, B. Auchmann, S. Kurz, V. Rischmuller, and S. Rjasanow. Edge-based BE-FE coupling for electromagnetics. 24(4):679–682, 2006.
[6] V. Rischmuller. *Eine Parallelisierung der Kopplung der Methode der finiten Elemente und der Randelementmethode*. PhD thesis, Universität Stuttgart, 2005.
[7] C. D. Villemagne and R. E. Skelton. Model Reduction using a Projection Formulation. *Int. J. Control*, 46:2141–2169, 1987.
[8] C. Voigt and J. Adamy. *Formelsammlung der Matrizenrechnung*. Oldenburg, 2007.